Talanta 117 (2013) 297–304

Contents lists available at ScienceDirect

Talanta

journal homepage: www.elsevier.com/locate/talanta

Simultaneous electrochemical determination of dopamine and paracetamol on multiwalled carbon nanotubes/graphene oxide nanocomposite-modified glassy carbon electrode

Srikanth Cheemalapati, Selvakumar Palanisamy, Veerappan Mani, Shen-Ming Chen *

Electroanalysis and Bioelectrochemistry Lab, Department of Chemical Engineering and Biotechnology, National Taipei University of Technology, No. 1, Section 3, Chung-Hsiao East Road, Taipei 106, Taiwan, ROC

ARTICLE INFO

Article history:
Received 1 July 2013
Received in revised form
25 August 2013
Accepted 26 August 2013
Available online 30 August 2013

Keywords:
Graphene oxide–multi-walled carbon nanotubes nanocomposite
Electrochemical determination
Dopamine
Paracetamol

ABSTRACT

In the present study, multiwalled carbon nanotubes (MWCNT)/graphene oxide (GO) nanocomposite was prepared by homogenous dispersion of MWCNT and GO and used for the simultaneous voltammetric determination of dopamine (DA) and paracetamol (PA). The TEM results confirmed that MWCNT walls were wrapped well with GO sheets. The MWCNT/GO nanocomposite showed superior electrocatalytic activity towards the oxidation of DA and PA, when compared with either pristine MWCNT or GO. The major reason for the efficient simultaneous detection of DA and PA at nanocomposite was the synergistic effect between MWCNT and GO. The electrochemical oxidation of DA and PA was investigated by cyclic voltammetry, differential pulse voltammetry and amperometry. The nanocomposite modified electrode showed electrocatalytic oxidation of DA and PA in the linear response range from 0.2 to 400 μmol L^{-1} and 0.5 to 400 μmol L^{-1} with the detection limit of 22 nmol L^{-1} and 47 nmol L^{-1} respectively. The proposed sensor displayed good selectivity, sensitivity, stability with appreciable consistency and precision.

1. Introduction

In recent years, neurotransmitters have received considerable interest due to its importance in the real life applications [1]. Among various neurotransmitters, dopamine (DA) is one of the main neurotransmitter which play a vital role in our central and peripheral nervous systems [2,3]. Acetaminophen or paracetamol (PA) is an important drug widely used for analgesics and antipyretics [4]. So far, various techniques have been employed for the detection of DA and PA, including high performance liquid chromatography (HPLC) [5], spectro-fluorimetry [6], mass spectrometry [7] and spectrophotometry [8]. However, the electrochemical methods are very simple, highly sensitive and less expensive than other time consuming traditional methods [9–11]. Nevertheless, the bare glassy carbon electrode (GCE) has poor sensitivity and selectivity towards the determination of DA and PA. In order to overcome these shortcomings, modified electrodes were employed with various materials, such as nanoparticles [12,13], polymers [14], metal oxides [15] and integrated nanomaterials [16]. Mostly, nanomaterials modified electrodes have been widely used for the simultaneous determination of different analytes, because of their exceptional properties such as fast electron transfer, high surface area, high stability and good biocompatibility. On the other hand, multiwalled carbon nanotube (MWCNT) has received considerable interest since its discovery, owing to its unique morphological features and electroanalytical properties [16–19]. So far, very few literature reports are available for the simultaneous detection of DA and PA by using MWCNT modified electrodes. For instance, functionalized MWCNT modified GCE [20] and hematoxylin-MWCNT modified carbon paste electrode [21] have been demonstrated for the simultaneous detection of DA and PA. Nevertheless, only MWCNT modified electrodes have fouling effect because of the accumulation of oxidized products on the electrode surface. With increasing advancements made in the field of nanotechnology, various nanomaterials have been incorporated with MWCNT using versatile approaches, leading to the preparation of novel nanocomposites to overcome the fouling effect.

Graphene oxide (GO), oxidative derivative of graphene have good biocompatibility, high electronic features and amphiphilic in nature distinct from other graphitic systems [22]. Owing to these unique advantages of GO, we used it to wrap MWCNT walls to form MWCNT/GO nanocomposite. Moreover, GO sheets have a high edge density (ρ_L) but lacks to maximize the edge density in 3D arrangement. On the other hand, MWCNT have high surface area 3D network, but contain lower surface charge density. Interestingly, the 3D network of GO–MWCNT nanocomposite

* Corresponding author. Tel.: +886 2270 17147; fax: +886 2270 25238.
E-mail address: smchen78@ms15.hinet.net (S.-M. Chen).

0039-9140/$ - see front matter © 2013 Elsevier B.V. All rights reserved.
http://dx.doi.org/10.1016/j.talanta.2013.08.041

could efficiently combine the high charge density of GO with high surface area of MWCNT to provide the highest edge density per unit nominal area. Thus, the highest edge density is one of the crucial reason for the superior performance of the GO/MWCNT nanocomposite than pristine GO or MWCNT [23]. Also there exists a great synergy between GO sheets and MWCNT, which also assist to harvest the excellent properties of two allotropes of carbon together and as a result exhibits high performance over GO or MWCNT alone [24,25]. Therefore, the superior performance of the GO/MWCNT nanocomposite can be explained by twofold, one is due to the synergy between GO and MWCNT and another is high edge density. The exceptional properties of MWCNT and GO could enhance the electron transfer as well as reduce the fouling effect of MWCNT. The unique properties of these two different nanometrials could enhance the electrocatalytic oxidation of DA and PA than only pristine GO or MWCNT.

In the present work, the simultaneous determination of DA and PA at MWCNT/GO nanocomposite has been reported. MWCNT/GO nanocomposite modified GCE displays good electrocatalytic oxidation towards DA and PA with well separated oxidation peaks for each species than only pristine MWCNT or GO. This could be ascribed to the synergistic effect of both MWCNT and GO. Moreover, the fouling effect of MWCNT modified electrode towards the oxidation of DA and PA has been addressed by using MWCNT/GO nanocomposite. The proposed sensor showed high sensitivity, selectivity with acceptable repeatability and reproducibility. The nanocomposite modified electrode displayed excellent recovery results for the simultaneous determination of DA and PA in commercially available real samples, revealing its good practicality.

2. Experimental

2.1. Materials

MWCNTs with the lengths of 0.1–10 μm were purchased from Aldrich. Graphite powder was obtained from Sigma-Aldrich. Dopamine hydrochloride and p-acetaminophen (BP-500 mg) were purchased from Sigma-Aldrich and used as received. The commercial samples of Dopamine hydrochloride and p-acetaminophen were purchased from O-Smart Company, Taiwan and Bristol Laboratories Ltd., UK, respectively. Commercially available dopamine hydrochloride injection (easy dopa injection 1.6 mg mL^{-1}) and Paracetamol tablets (BP 500 LC) were diluted with PBS prior to the analysis of DA and PA. Aliquots of these diluted samples were spiked into the PBS and diluted urine samples for the individual and simultaneous determination of DA and PA using the modified electrode. Prior to the analysis, all the samples were diluted with pH 7 (0.5 mmol L^{-1} PBS) solution and aliquots of these diluted samples were used for DPV analysis. Human urine sample aliquots were obtained from two healthy men and the samples were stored in a refrigerator at 4 °C. About 25 ml of urine samples were centrifuged for 15 min at 3000 rpm. After that each 1 ml of the supernatant was collected and further diluted 10 times with PBS to reduce the complex interference present in the urine. The solutions were attentively transferred into the 25 ml electrochemical cell and analyzed without any further pretreatment. Recovery values were calculated using the formula: Recovery (%)=(added/found) × 100. Here, added and found values are the concentrations of the analyte spiked into the solution and that had been determined. The supporting electrolyte used for all the experiments was pH 7 (0.05 mol L^{-1} PBS), prepared by using 0.05 mol L^{-1} Na_2HPO_4 and NaH_2PO_4. All the other pH solutions were adjusted with 0.5 mol L^{-1} H_2SO_4 and 2 mol L^{-1} NaOH. All the chemicals used in this study were of analytical grade and used without any further purification.

2.2. Instrumentation

Cyclic voltammetry (CV) and differential pulse voltammetry (DPV) studies were performed using CHI 1205 and CHI 450a work stations, respectively. Transmission electron microscopy (TEM) study was performed using JEM 2007 model transmission electron microscope. Raman spectra were recorded using a Raman spectrometer (Dong Woo 500i, Korea) equipped with a charge-coupled detector. Amperometric (i–t curve) measurements were performed using a CHI-750a potentiostat with an analytical rotator AFMSRX (PINE instruments, USA). Electrochemical impedance spectroscopy (EIS) studies were performed using IM6ex ZAHNER (Kronach, Germany). A conventional three-electrode system consisting of a modified GCE as a working electrode (active surface area = 0.079 cm^{-2}), an Ag/AgCl electrode (Sat. KCl) as a reference electrode and a platinum wire with 0.5 mm diameter as a counter electrode was employed in electrochemical experiments. All the electrochemical measurements were carried out at room temperature and electrolyte cell solutions were kept under a nitrogen (N_2) atmosphere.

2.3. Fabrication of MWCNT/GO nanocomposite modified GCE

GO was prepared by the Hummer's method [23]. As prepared, purified graphite oxide was exfoliated by bath sonication for 2 h to obtain GO. To prepare MWCNT/GO nanocomposite, MWCNT was added into 0.5 mg/mL of GO aqueous solution (1:2, V:V %) and sonicated for 45 min to produce a homogeneous dispersion, which has been considered as the most common way to disperse MWCNT with GO in water [24,25]. Finally, the MWCNT/GO nanocomposite was centrifuged at 3000 rpm to remove the loosely bound MWCNTs and washed several times with water. The as-purified MWCNT/GO composite was dried overnight, redispersed in water and used for the further experiments.

Prior to modification, GCE was polished with alumina slurry and slightly sonicated for about 2 min in ethanol and water (1:1) mixture. Then, the cleaned GCE surface was dried at room temperature. About 8 μl (optimized concentration) of the MWCNT/GO dispersion was drop casted on GCE surface and dried at ambient temperature. Thus obtained MWCNT/GO nanocomposite modified GCE surface was gently washed with water to remove the loosely attached MWCNT/GO composite and used further. The MWCNT/GO modified GCE was stored at 4 °C under dry condition when not in use.

3. Results and discussion

3.1. Characterization of MWCNT/GO nanocomposite

Surface morphological characterization of MWCNT/GO nanocomposite was studied by using TEM analysis. The TEM morphology of pristine MWCNT (inset of Fig. 1A) depicts tubular structures of diameter ranging from 30 to 50 nm, a characteristic morphology of MWCNT. Whereas, GO was observed like an ultra thin flat sheet, having a diameter of nanometers to sub micrometer (S1). The TEM image of MWCNT/GO nanocomposite (Fig. 1A) shows that MWCNT walls were wrapped well with thin sheets of GO [26,27]. This could be due to the π–π stacking interaction between the sidewalls of MWCNT and hydrophobic regions of GO. Fig. 1B shows the Raman spectrum of MWCNT (a), GO (b) and MWCNT/GO (c). The D and G band values of MWCNT and GO observed in this study were similar to the D and G band values for MWCNT and GO reported previously [24]. Moreover, the intensity ratio of D-band to G-band (I_D/I_G) was estimated for MWCNT/GO nanocomposite before and after the introduction of MWCNT into GO solution. The I_D/I_G band ratio (0.87) was slightly decreased when compared

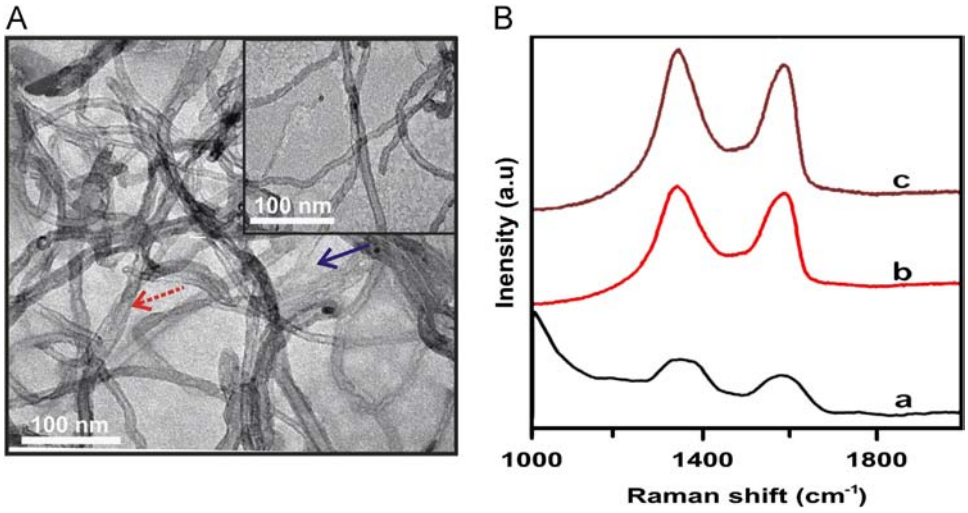

Fig. 1. (A) TEM images of MWCNT/GO nanocomposite and MWCNT (inset). The arrow indicates the MWCNT (dotted arrow) and GO (continuous arrow). (B) Raman spectrum of MWCNT (a), GO (b) and MWCNT/GO nanocomposite (c).

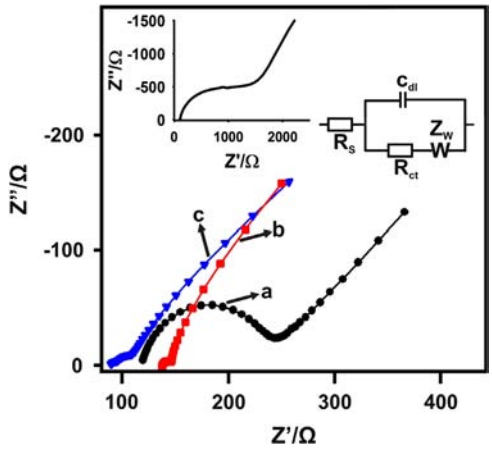

Fig. 2. EIS of bare (a), MWCNT (b), GO (inset) and MWCNT/GO nanocomposite (c) modified GCEs in 5 mmol L^{-1} $Fe(CN)_6^{3-/4-}$ containing PBS. Inset is the Randles equivalent circuit. R_s, C_{dl}, R_{ct} and Z_w represents the resistance of the electrolyte solution, double layer capacitance, charge-transfer resistance and the Warburg impedance, respectively. The frequency range used is from 0.1 Hz to 100 kHz.

with pristine MWCNT (88.2) or GO (0.94). We also observed a red shift of the peak positions at the nanocomposite confirming the effective formation of MWCNT/GO nanocompsoite [24]. Similarly, the Raman spectrum of GO exhibits D and G bands with intensities quite higher than that of MWCNT, since extensive oxidation at the graphitic systems renders the reduction of planed sp^2 domains. However, intensity ratio of D and G bands have been increased after the formation of the MWCNT/GO nanocomposite.

EIS has been used to monitor the electrochemical impedance changes at the different film modified GCEs. Fig. 2 shows the EIS of bare (a), MWCNT (b), MWCNT/GO and GO (inset) (c) modified GCEs in PBS containing 5 mmol L^{-1} $Fe(CN)_6^{3-/4-}$. Fig. 2 inset shows the Randles equivalent circuit model, where the equivalence circuit parameters such as R_{et}, R_s, C_{dl} and Z_w represents the electron transfer resistance, solution transfer resistance, double layer capacitance and Wardburg impedance, respectively. The total electrode impedance consists of the R_s in series with the parallel connection of the C_{dl} and Z_w. The semicircular part diameter is equivalent to the electron transfer resistance. The linear part at lower frequencies corresponds to the diffusion process. A semicircle portion results from the parallel combination of electron transfer resistance (R_{et}) and C_{dl} resulting from electrode impedance [23]. The same solution was used throughout all EIS measurements to maintain the solution resistance (R_s) constant. The bare GCE exhibited a depressed semicircle with an R_{ct} value of 110 Ω when compared with GO modified GCE (567 Ω), revealing the hindered electron transfer at GO modified electrode. By contrary, MWCNT modified GCE showed a depressed semicircle with R_{ct} value of 7.6 Ω, validating its high conductivity and fast electron conducting ability at the electrode surface. Whereas, there is a slight increment in the R_{ct} value (9.0 Ω) at the nanocomposite electrode, due to the presence of GO in the nanocompsoite modified electrode. The R_s of each modified electrode were shifted slightly to the higher portions (20–50 Ω), the reason may be due to the semicircle portion of the former has been slightly shifted towards higher frequency. However, the semicircle diameter remains unchanged, thus the presence of MWCNT sustains the electron transfer process at the nanocomposite modified electrode. The rapid electron transfer at the nanocomposite can be ascribed to the excellent conductivity of MWCNT, which acts as a good conduit between GO and the electrode surface. We also performed UV–vis spectra to confirm the π–π stacking interaction is formed between GO and MWCNT. In UV–vis spectrum GO exhibits two characteristic peaks: a shoulder peak at 231 nm and a broad peak at 300 nm, which are assigned to the π–π* and n–π* transitions, respectively (figure not shown). The composite also exhibits two similar absorption peaks, while the position of the π–π* peak bathochromically shifted to 246 nm, confirming that π–π stacking interaction is formed between GO and MWCNT consistent with the TEM results [24,26].

3.2. Cyclic voltammetry of DA and PA at MWCNT/GO nanocomposite modified electrode

Fig. 3 shows the CVs of different modified GCEs at the scan rate of 50 mV in pH 7 (PBS) containing 20 μmol L^{-1} of DA and 30 μmol L^{-1} of PA at bare (curve a), GO (curve b), MWCNT (curve c), and MWCNT/GO (curve d) modified GCEs. Cyclic voltammograms were recorded in the potential range of −0.2 to 0.8 V. Well defined symmetric redox peaks for both DA and PA were observed at various modified electrodes, which ascribed to oxidation of DA and PA at the electrode surface. At the bare GCE, broad oxidation peaks were observed at 0.344 and 0.550 V for DA and PA respectively. Likewise, at GO modified GCE, the oxidation peak of DA and PA appeared broadly at 0.247 and 0.445 V. Whereas, at MWCNT modified GCE, the oxidation peaks for DA and PA were observed at 0.215 and 0.410 V respectively. Albeit, at MWCNT modified electrode for the

detection of DA and PA, serious fouling effect was observed at the electrode surface during the measurements, which was caused by the fouling and the accumulation of the oxidized by-products on the electrode surface and it was discussed in detail in Section 3.5.

Nonetheless, bare and GO modified GCEs showed a poor sensitivity towards DA and PA and the corresponding oxidation peak currents are relatively very small. While, at MWCNT/GO modified GCE well defined oxidation peaks of DA and PA appeared at 0.204 and 0.408 V with peak to peak separation (ΔE_p) values of 46 and 49 mV respectively. ΔE_p denotes the separation between the anodic and cathodic peak potentials (E_{pc}–E_{pa}). The smaller ΔE_p values revealed the faster electron transfer of DA and PA at the electrode surface. Additionally, the oxidation peak currents of DA and PA observed at the nanocomposite electrode were 8- and 5-fold higher than those observed at GO and MWCNT modified electrodes, respectively. The notable enhancements in the oxidation peak currents of DA and PA can be ascribed to the synergistic effect of MWCNT and GO that have played an important role in facilitating the direct electron transfer of DA and PA at the electrode surface. Additionally, the decrease in over potential, smaller peak to peak separation values and higher oxidation currents of DA and PA indicates that nanocomposite modified electrode has a promising electrocatalytic oxidation towards the DA and PA. A typical schematic representation for the oxidation of DA and PA at MWCNT/GO nanocomposite modified GCE are shown in Fig. 4.

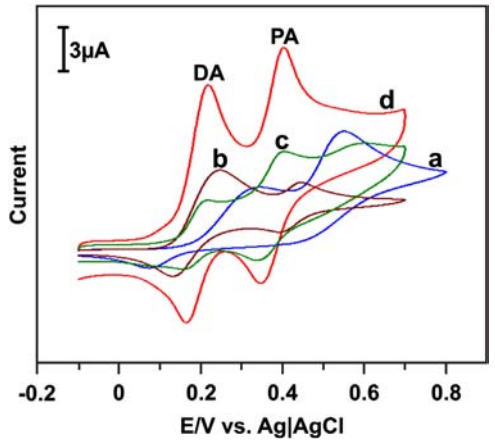

Fig. 3. (A) Cyclic voltammograms of bare GCE (a), MWCNT (b), GO (c) and MWCNT/GO film modified GCEs in 20 μmol L^{-1} of DA and 30 μmol L^{-1} of PA at 50 mV s^{-1} scan rate.

Fig. 5A and B shows the cyclic voltammograms of MWCNT/GO nanocomposite film modified GCE in deoxygenated PBS containing 30 μmol L^{-1} PA and 20 μmol L^{-1} DA respectively, at various scan rates. Upon increasing the scan rates, the anodic and cathodic peak currents and ΔE_p values increased linearly. Meanwhile, the peak potentials shifted slightly. Both anodic and cathodic peak currents increased linearly when the scan rates were increased from 50 to 500 mV s^{-1} (Fig. 5A′ and B′). The peak potentials shifted slightly towards the positive and negative direction at higher scan rates, suggesting that DA and PA oxidation processes at the MWCNT/GO nanocomposite electrode is a surface-controlled not diffusion controlled [28].

3.3. Simultaneous determination of DA and PA at MWCNT/GO nanocomposite film modified electrode

CV studies were used to investigate the simultaneous determination of DA and PA at MWCNT/GO nanocomposite film modified electrode in the potential range of −0.2 to 0.8 V at the scan rate of 50 mV s^{-1} (Fig. 6A). It can be seen that two well resolved anodic peaks were observed at 0.204 and 0.408 V for DA and PA, respectively with ΔE_p of 204 mV, indicating the efficient simultaneous determination of DA and PA. The oxidation peak currents for each DA and PA concentrations were measured separately from the corresponding oxidation peaks in CV after performing baseline corrections. Moreover, the oxidation peak currents of DA and PA increased linearly with increasing DA and PA concentrations from 0.2 to 400 μmol L^{-1} (inset in Fig. 6A) with the correlation coefficients of 0.976 and 0.957, respectively.

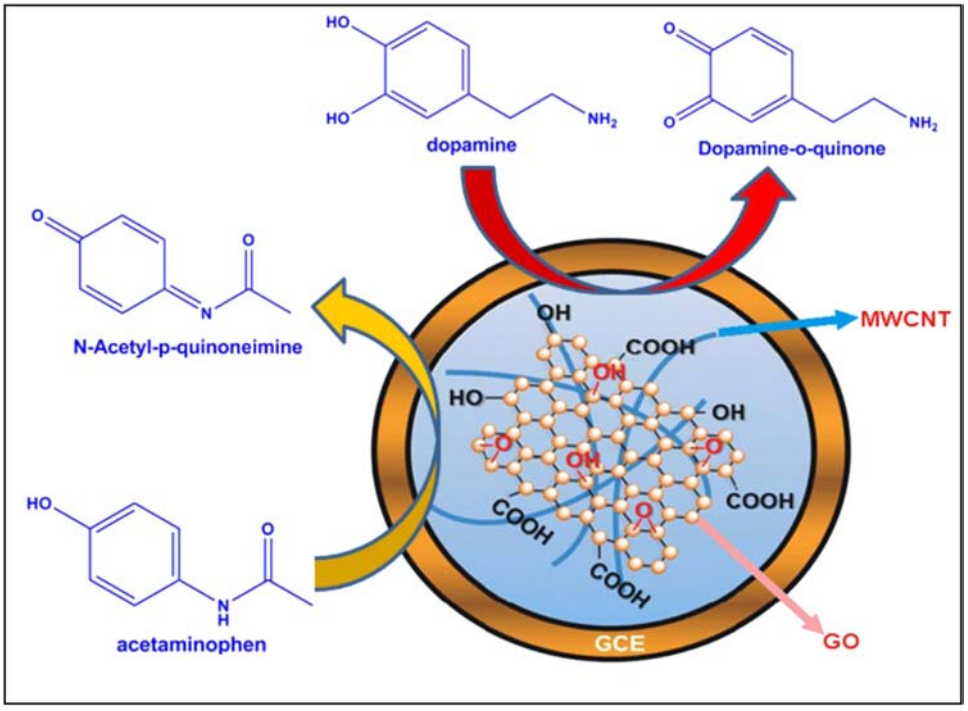

Fig. 4. A schematic representation for the typical electrooxidation of DA and PA at MWCNT/GO nanocomposite modified GCE.

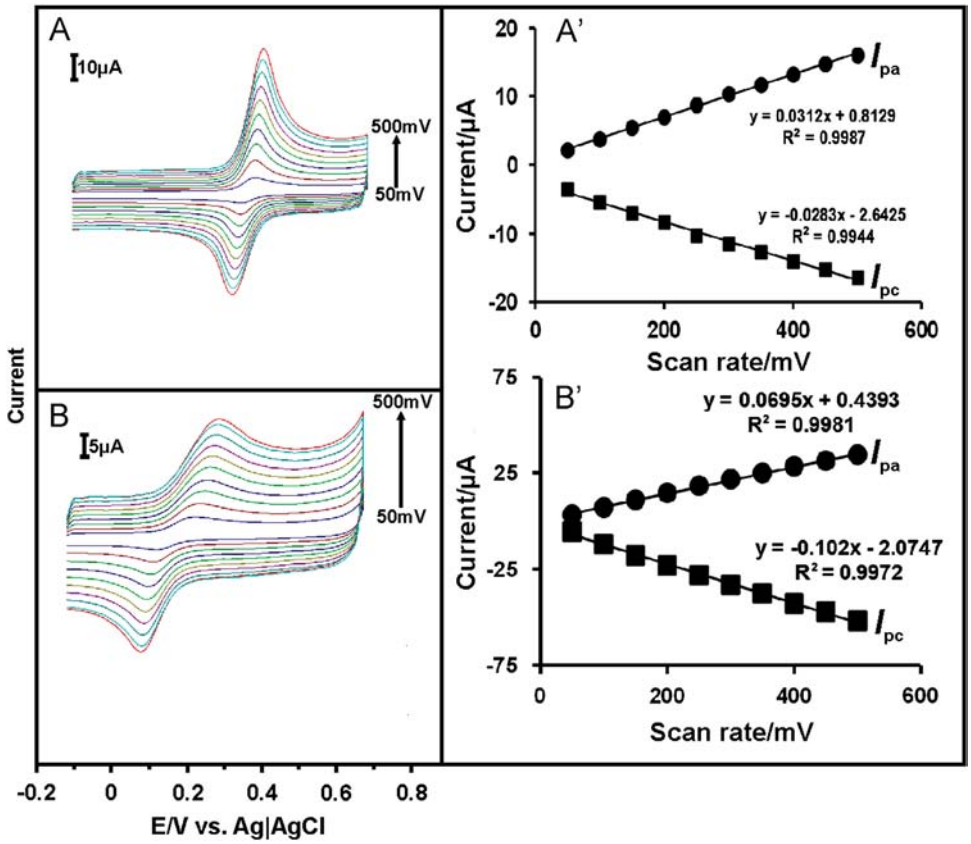

Fig. 5. (A) Cyclic voltammograms recorded at MWCNT/GO film modified GCE in 30 μmol L^{-1} of PA in deoxygenated PBS at different scan rates. The scan rates from inner to outer are: 50 to 500 mV s^{-1}. A′ shows the linear dependence of I_{pa} and I_{pc} on scan rate (50 to 500 mV s^{-1}). (B) Cyclic voltammograms recorded at MWCNT/GO film modified GCE in 20 μmol L^{-1} of DA in deoxygenated PBS at different scan rates. The scan rates from inner to outer are: 50 to 500 mV s^{-1}. B′ shows the linear dependence of I_{pa} and I_{pc} on scan rate (50 to 500 mV s^{-1}).

Fig. 6B shows the DPVs obtained at MWCNT/GO nanocomposite film modified electrode for different DA and PA concentrations in pH 7 (0.05 M PBS). The oxidation peak currents for different concentrations of DA and PA were measured separately from the corresponding oxidation peaks in DPV after performing baseline corrections. The corresponding anodic currents of DA and PA increased linearly with increasing the concentrations of DA and PA with a ΔE_p value was 0.204 V (inset in Fig. 6B). The anodic peak current of DA and PA increased linearly over the range of 200 nmol L^{-1} to 400 μmol L^{-1} with the correlation coefficient of 0.99 and 0.987, respectively. The sensitivity was calculated from the fitted regression equation as 1.53 and 0.938 μA μmol L^{-1} cm^{-2} for DA and PA, respectively.

Moreover, the cross reactivity of two analytes has also been investigated by LSV, and the corresponding figure has been shown in Fig. S2. From the LSV results, the two analytes did not have any cross reactivity with each other and it would be a great asset for the simultaneous determination of DA and PA. The promising catalytic activity of the nanocomposite can be ascribed to the surface negative charges due to the presence of COOH groups at basal plane of the GO, which easily attracts the positively charged DA (pKa = 8.9) PA (pKa = 9.5) species towards the electrode surface [20]. Table 1 shows the analytical performance (linear range and limit of detection) of the proposed sensor was compared with other carbon nanomaterials modified DA and PA sensors. Table 1 was evident that the proposed sensor has a wider linear range and low LOD (except graphene modified electrode) than previously reported other carbon nanomaterials modified electrodes for DA and PA. Moreover, the analytical performance of this sensor for PA is comparable with graphene modified electrodes. The superior performance of the GO/MWCNT nanocomposite showed a promising platform for the simultaneous electrochemical determination of DA and PA.

3.4. Amperometric studies

Amperometric i–t technique is the most reliable and sensitive method to evaluate the electrocatalytic activity of DA and PA at MWCNT/GO nanocomposite film modified rotating disc electrode (RDE). Fig. 6C and D shows the typical i–t plots for the MWCNT/GO nanocomposite film modified GCE under the optimized experimental conditions with the successive addition of different concentrations of DA and PA into N_2 saturated constantly stirred PBS (pH 7) at different time intervals. The working potential was hold at 0.204 V for DA and 0.408 V for PA. After the current became stable, different concentrations of DA (3 μM, 10 μM and 15 μM) (Fig. 6C) and PA (5 μM, 10 μM and 20 μM) (Fig. 6D) were injected into the continuously stirred PBS (pH 7), and their corresponding responses were measured. It can be seen that a good amperometric response current was observed for the successive additions of 1 μM of DA and PA (inset lower in Fig. 6C and D), validating that the rapid electrooxidation of DA and PA at MWCNT/GO nanocomposite modified electrode surface. The response current reaches its 95% steady state current within 3 s for DA and 5 s for PA, validating the rapid catalytic oxidation processes that have occurred at the composite electrode surface. The response currents of DA and PA increased linearly over the entire concentrations ranging from 0.1 to 400 μmol L^{-1} and 0.2 to 400 μmol L^{-1}, with the correlation coefficients of 0.991 and 0.997, respectively. The MWCNT/GO nanocomposite film modified electrode showed sensitivity values of 0.656 and 0.529 μA μmol L^{-1} cm^{-1} for DA and PA, respectively

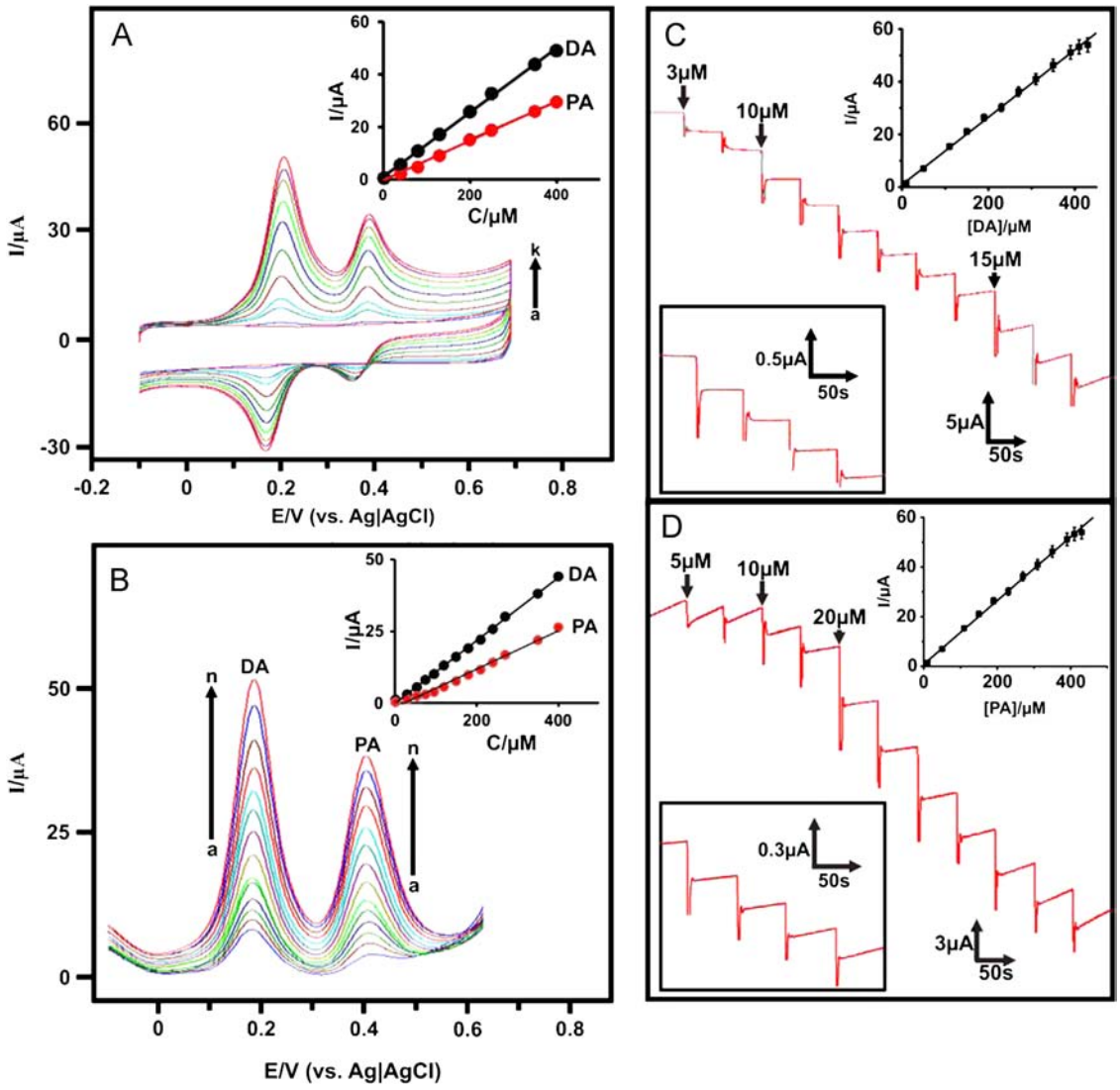

Fig. 6. (A) CVs of MWCNT/GO nanocomposite film modified GCE (a) without and (b–k) with 200 nmol L^{-1}–400 μmol L^{-1} of DA and PA containing deoxygenated PBS at 50 mV s^{-1} scan rate. Inset plot shows the linear dependence of I_{pa} vs. [DA] and [PA]. (B) DPVs recorded at MWCNT/GO nanocomposite film modified GCE (a) without and (b–n) with 200 nmol L^{-1}–400 μmol L^{-1} of DA and PA containing deoxygenated PBS at 50 mV s^{-1} scan rate. Inset plot shows the linear dependence of I_{pa} vs. [DA] and [PA]. (C) Amperometric *i–t* response at MWCNT/GO nanocomposite film modified rotating disc GCE upon successive additions of 100 nmol L^{-1}–400 μmol L^{-1} of DA into continuously stirred N_2 saturated PBS (pH 7). Applied potential: 0.204 V; inset (upper) shows the calibration curve of I_{pa} vs. [DA]. Inset (bottom) shows *i–t* response for each addition of 1 μM of DA. (D) Amperometric responses acquired under similar conditions for successive additions of 200 nmol L^{-1}–400 μmol L^{-1} of PA. Applied potential of 0.408 V; inset (upper) shows the calibration curve of I_{pa} vs. [PA]. Inset (bottom) shows *i–t* response for each addition of 1 μM of PA.

Table 1
Comparison of the analytical performance of the proposed electrode with previously reported carbon nanomaterials modified electrodes for DA and PA.

Modified electrode	DA (LOD[a]) (μmol L^{-1})	PA (LOD) (μmol L^{-1})	DA (LR[b]) (μmol L^{-1})	PA (LR) (μmol L^{-1})	Reference
MWCNT[c]/GO[d]	0.02	0.05	0.2–400	0.5–400	This work
f-MWCNT[e]	0.8	0.6	3–200	3–300	[20]
MWCNT/GONR[f]	0.08	NA[g]	0.15–12.15	NA	[29]
Graphene	NA	0.032	NA	0.1–20	[30]
Pyrolytic carbon	2.3	1.4	18–270	15–225	[31]
SWCNT[h]	0.048	0.076	3–200	0.5–100	[32]

[a] LOD – Limit of detection.
[b] LR – Linear range.
[c] MWCNT – Multiwalled carbon nanotubes.
[d] GO – Graphene oxide.
[e] f-MWCNT – Functionalized multiwalled carbon nanotubes.
[f] GONR – Graphene oxide nanorods.
[g] NA – Not available.
[h] SWCNT – Single walled carbon nanotubes.

with limit of detection (LOD) values of 22 and 47.2 nmol L^{-1} ($S/N=3$). The excellent electrocatalytic activity of DA and PA at the proposed sensor is attributed to the synergistic effect and good biocompatibility of MWCNT and GO.

3.5. Electrode fouling

In the electroanalytical chemistry, either composite or bare modified electrodes have been used for sensing of different analytes. The each modified electrode has attracted by different analytes with unique way, possibly leads to the unexpected reactions or fouling of the signal. Hence, the accuracy of reproducible results of the electrodes is more considered when they used more than one time in the same analyte. Fig. S3 shows the DPV of electrooxidation of DA and PA at GO/MWCNT (a) and MWCNT (b) modified electrodes in the presence of 20 μmol L^{-1} DA and 50 μmol L^{-1} PA at 50 mV s^{-1}. GO/MWCNT nanocomposite modified electrode shows a constant current response of DA (RSD=0.26) and PA (RSD=0.69) at four different runs in same potential window. Whereas, MWCNT modified electrodes shows serious current decrement for the oxidation peak current of DA (RSD=3.26) and PA (RSD=7.8), which is caused by the adsorption of oxidized products of DA and PA on the MWCNT electrode surface. This result clearly demonstrates that the MWCNT/GO nanocomposite could use for the accurate detection of DA and PA than MWCNT modified electrode.

3.6. Anti-interference studies

It is well known that ascorbic acid (AA), uric acid (UA) and NADH are coexisting with DA and PA in biological fluids [33,34]. We investigated the possible interference of these biologically active species using amperometric *i–t* technique (Fig. S4A and B). Thus we monitored the response current against each addition of 20 μmol L^{-1} of DA (Fig. S4A) and 50 μmol L^{-1} of PA (Fig. S4B) in the presence of 0.2 mmol L^{-1} solutions of each AA (pKa=4.3), UA (pKa=5.4) and NADH ((pKa=5.6) at different time intervals. Other experimental conditions are same as that mentioned in Section 3.4. No noteworthy response current was observed for each addition of the interfering species, because they are repelled well by the negatively charged MWCNT/GO nanocomposite surface [20,33]. It was concluded that, interfering effect caused by these electroactive species is quite negligible, validating that simultaneous determination of DA and PA is highly selective at the MWCNT/GO nanocomposite film.

3.7. Real sample analysis

To evaluate the feasibility of the proposed sensor, the selective determination of DA and PA in real samples is highly requisite. The analytical performance of the proposed electrode was investigated in pharmaceutical and urine sample results and the recovery results are summarized in Tables 2 and 3. The good recovery results of spiked samples of DA in injections and PA in tablets validating that this proposed MWCNT/GO nanocomposite electrode could be used for the effective determination of DA and PA in both pharmaceutical samples and urine samples. The promising futures of the nanocomposite could be ascribed by the high stability and synergistic effect of MWCNT/GO nanocomposite.

3.8. Stability, repeatability and reproducibility

In order to investigate the storage stability of proposed sensor, MWCNT/GO nanocomposite modified electrode was stored in N_2 saturated PBS containing 100 μmol L^{-1} of DA and PA at 4 °C and 27 ºC. The sensitivity of the modified electrode was monitored periodically up to one week using CV. The modified electrode retained about 91.3% of DA and PA initial sensitivity at 4 °C and 89.6% at 27 °C in one week, indicating the excellent storage stability of the sensor. The repeatability and reproducibility of the proposed sensor were evaluated by CV studies. The five electrodes fabricated independently showed an acceptable precision with a relative standard deviation (RSD) of 4.23 for 100 μmol L^{-1} DA and PA

Table 2
Determination of DA and PA in pharmaceutical samples.

Quantitative analyses of DA and PA in the samples	Sample	Added (μmol L^{-1})		Found (μmol L^{-1})		Recovery (%)		RSD[a] (%)	
		DA	PA	DA	PA	DA	PA	DA	PA
Dopamine hydrochloride injection	1	100	–	100.03		100.03		1.97	
	2	200	–	200.04		100.02		2.75	
Paracetamol tablet	1	–	100		99.93		99.93		4.94
	2	–	200		199.97		99.98		2.12

1 and 2 spiked diluted pharmaceutical samples of DA and PA in PBS.
[a] Relative standard deviation of three measured values.

Table 3
Determination of mixtures of DA and PA in urine samples at MWCNT/GO nanocomposite modified electrode ($n=3$).

Sample	Added (μM)		Detected[a] (μM)		Recovery (%)		RSD (%)	
	DA	PA	DA	PA	DA	PA	DA	PA
Dopamine hydrochloride injection (1.6 mg mL^{-1})	–	–	10.2	–	–	–	–	–
Paracetamol tablet (BP 500)	–	–	–	55.5	–	–	–	–
1	50	50	60.5	105.3	100.4	99.8	2.23	1.47
2	75	75	84.0	129.9	98.6	99.5	3.53	2.18
3	100	100	108.9	155.7	98.8	101.1	3.22	2.74

1, 2 and 3 spiked diluted pharmaceutical samples of mixtures of DA and PA in urine.
[a] Standard addition method.

concentration measurements. The RSD for 10 successive measurements of each 100 μmol L^{-1} DA and PA is 3.9 revealing the good consistency of the proposed sensor.

4. Conclusions

In conclusions, MWCNT/GO nanocomposite was prepared simply by simple sonication of MWCNT with GO aqueous solution. The strong π–π stacking interactions between MWCNT and GO provides good stability to the dispersion. The fouling of pristine MWCNT modified electrodes was resolved by using MWCNT/GO modified electrode. The good biocompatibility and synergistic effect of GO and MWCNT showed an enhanced sensitivity and low LOD for DA and PA. Besides, nanocomposite film modified electrode exhibits good sensitivity, selectivity, with acceptable storage stability. The practicality of the proposed sensor was evaluated by sensing DA and PA in pharmaceutical and human urine samples with good recovery results.

Acknowledgments

This work was supported by the National Science Council and the Ministry of Education of Taiwan, Republic of China. The authors express their gratitude to Dr. Arun Prakash Periasamy and Mr. Prathik Roy for their timely help and valuable suggestions throughout this project.

Appendix A. Supplementary material

Supplementary data associated with this article can be found in the online version at http://dx.doi.org/10.1016/j.talanta.2013.08.041.

References

[1] J. Ping, J. Wu, Y. Wang, Y. Ying, Biosens. Bioelectron. 34 (2012) 70–76.
[2] R.A. Wise, Nat. Rev. Neurosci. 5 (2004) 483–494.
[3] G.A. Evtugyn, R.V. Shamagsumova, R.R. Sitdikov, I.I. Stoikov, I.S. Antipin, M.V. Ageeva, T. Hianik, Electroanalysis 23 (2011) 2281–2289.
[4] X. Chen, J. Zhu, Q. Xi, W. Yang, Sens. Actuators B 161 (2012) 648–654.
[5] J.M. Wilson, J.T. Slattery, A.J. Forte, S.D. Nelson, J. Chromatogr. B: Biomed. Sci. Appl. 227 (1982) 453–462.
[6] H.Y. Wang, Y. Sun, B. Tang, Talanta 57 (2002) 899–907.
[7] H.C. Curtius, M. Wolfensberger, B. Steinmann, U. Redweik, J. Siegfried, J. Chromatogr. A 99 (1974) 529–540.
[8] M. Mamiński, M. Olejniczak, M. Chudy, A. Dybko, Z. Brzózka, Anal. Chim. Acta 540 (2005) 153–157.
[9] Y. Umasankar, B. Unnikrishnan, S.M. Chen, T.W. Ting, Int. J. Electrochem. Sci. 7 (2012) 484–498.
[10] R.N. Goyal, V.K. Gupta, M. Oyama, N. Bachheti, Electrochem. Commun. 7 (2005) 803–807.
[11] X. Cao, L. Luo, Y. Ding, X. Zou, R. Bian, Sens. Actuators B 129 (2008) 941–946.
[12] C.R. Raj, T. Okajima, T. Ohsaka, J. Electroanal. Chem. 543 (2003) 127–133.
[13] S. Reddy, B.E.K. Swamy, H. Jayadevappa, Electrochim. Acta 61 (2012) 78–86.
[14] U. Lange, N.V. Roznyatovskaya, V.M. Mirsky, Anal. Chim. Acta 614 (2008) 1–26.
[15] W.D. Zhang, B. Xu, L.C. Jiang, J. Mater. Chem. 20 (2010) 6383–6391.
[16] Z. Zhuang, J. Li, R. Xu, D. Xiao, Int. J. Electrochem. Sci. 6 (2011) 2149–2161.
[17] Q. Zhao, Z. Gan, Q. Zhuang, Electroanalysis 14 (2002) 1609–1613.
[18] C.B. Jacobs, M.J. Peairs, B.J. Venton, Anal. Chim. Acta 662 (2010) 105–127.
[19] Y. Zhang, X. Sun, L. Zhu, H. Shen, N. Jia, Electrochim. Acta 56 (2011) 1239–1245.
[20] Z.A. Alothman, N. Bukhari, S.M. Wabaidur, S. Haider, Sens. Actuators B 146 (2010) 314–320.
[21] H.R. Zare, N. Nasirizadeh, Int. J. Electrochem. Sci. 4 (2009) 1691–1705.
[22] D.R. Dreyer, S. Park, C.W. Bielawski, R.S. Ruoff, Chem. Soc. Rev. 39 (2010) 228–240.
[23] W.S. Hummers, R.E. Offeman, J. Am. Chem. Soc. 80 (1958) 1339.
[24] S.H. Aboutalebi, A.T. Chidembo, M. Salari, K. Konstantinov, D. Wexler, H.K. Liu, S.X. Dou, Energy Environ. Sci. 4 (2011) 1855–1865.
[25] Y. Li, T. Yang, T. Yu, L. Zheng, K. Liao, J. Mater. Chem. 21 (2011) 10844–10851.
[26] Q. Zhang, S. Yang, J. Zhang, L. Zhang, P. Kang, J. Li, J. Xu, H. Zhou, X.M. Song, Nanotechnology 22 (2011) 494010.
[27] L. Zhang, H. Zhang, R. Zhou, Z. Chen, Q. Li, S. Fan, G. Ge, R. Liu, K. Jiang, Nanotechnology 22 (2011) 385704.
[28] I. Streeter, G.G. Wildgoose, L. Shao, R.G. Compton, Sens. Actuators B 133 (2008) 462–466.
[29] C.L. Sun, C.T. Chang, H.H. Lee, J. Zhou, J. Wang, T.K. Sham, W.F. Pong, ACS Nano 5 (2011) 7788–7795.
[30] X. Kang, J. Wang, H. Wu, J. Liu, I.A. Aksay, Y. Lin, Talanta 81 (2010) 754–759.
[31] G.P. Keeley, N. McEvoy, H. Nolan, S. Kumar, E. Rezvani, M. Holzinger, S. Cosnier, G.S. Duesberg, Anal. Methods 4 (2012) 2048–2053.
[32] B. Habibi, M. Jahanbakhshi, M.H.P. Azar, Electrochim. Acta 56 (2011) 2888–2894.
[33] P. Kalimuthu, S.A. John, Bioelectrochemistry 77 (2009) 13–18.
[34] S. Palanisamy, S. Cheemalapati, S.M. Chen, Anal. Biochem. 429 (2012) 108–115.